



Research Article

Synergistic effect of h-BN on thermal conductivity of polymer compositesNilay Kucukdogan ^{a,*} ^aDepartment of Mechatronics Engineering, Manisa Celal Bayar University, Manisa, Turkey

ARTICLE INFO

Article history:

Received 25 July 2022

Accepted 01 November 2022

Published 15 December 2022

Keywords:

Bruggeman model

Boron nitride

Multi walled carbon nanotube

Polymer composite

ABSTRACT

The conductivity characteristics of polymers and polymer composites have become more significant recently. Good heat dissipation is required in many applications, such as circuit boards and heat exchangers, so it is essential to develop the thermal conductivity characteristics of the materials. The micro-fillers have been replaced with nano or hybrid fillers to increase the low thermal conductivity of the polymer. Hexagonal boron nitride (h-BN) and multi-walled carbon nanotubes (MW-CNT), both of which have good conductivity properties, are two popular filling materials. The presence of hydroxyl and amino active groups at the corners of the hexagonal structure of BN improves the thermal conductivity properties of the polymer composite. In addition, it shows high thermal conductivity behavior in polymer composite structures with BN and MW-CNT. It is essential to demonstrate the effects of the volume fraction of additives on the thermal properties of composites with various approaches. In this study, the thermal conductivity behaviors of h-BN/high-density polyethylene and h-BN/MW-CNT/high-density polyethylene composites are demonstrated using the theoretical Bruggeman model, which is based on the assumption that there are constant infinitesimal changes in the material so that there is an interaction between particles. The coefficient of determination (R^2) between the thermal conductivity values of the composites and the predictions of the Bruggeman theoretical model is greater than 0.98. This way, the synergetic effect of h-BN and MW-CNT/h-BN additives on thermal conductivity has been theoretically proven.

1. Introduction

Due to their electrical insulation, corrosion resistance, lightweight, simple and low energy requirement manufacturing, and low cost, polymer composite, a material that is frequently used in electronic packages, has drawn growing interest. In addition, effective heat dissipation has emerged as a critical issue for the everyday operation of electronics due to the rapid growth of electronic devices toward downsizing, portability, and integration. Improvements are being made to polymer composites' thermal conductivity to better manage and control heat dissipation in electronic devices. One of the most popular methods is adding materials with high conductivity filling material into the polymer structure. However, it has also been demonstrated that adding these materials in various sizes as filler material contributes to increased heat conductivity. First, filling materials used in micron sizes were left to nano and hybrid additive materials [1, 2]. The thermal conductivity of polymer composites is related to the polymer, fillers, and their

interactions. Here, it can change with the morphology, size, shape, and orientation of the fillers in the polymer structure and the formation of the interface or interphase with the polymer. Many parameters should be considered in the design of polymer composites with thermal conductivity. Selecting suitable polymers and fillers alone is not enough. The morphology and interaction of polymers and fillers must also be considered [3].

Metals with high thermal conductivity (copper, silver, zinc) [4] or metal oxides (alumina) [5, 6] and carbon-based [7] fillers increase the thermal conductivity of polymer composites. Among these, it has been demonstrated that good mechanical properties are obtained in addition to excellent thermal conductivity, especially in additive materials such as MW-CNT, fullerene, graphene, and boron nitride [8]. These carbon-based filler materials rapidly transfer electrons and phonons in their direction with little scattering. For this reason, the thermal conductivity of the produced composites is presented in two ways: in-plane and through-plane. When investigated

* Corresponding author. Tel.: +90 236 314 1010; Fax: +90 236 314 2020.

E-mail addresses: nilay.ozturk@cbu.edu.tr (N. Kucukdogan)

ORCID: 0000-0003-4375-0752 (N. Kucukdogan)

DOI: [10.35860/iarej.1148320](https://doi.org/10.35860/iarej.1148320)© 2022, The Author(s). This article is licensed under the CC BY-NC 4.0 International License (<https://creativecommons.org/licenses/by-nc/4.0/>).

depending on the volume fraction, very different results have been revealed in polymer composites in both directions. Zhang et al. presented an easy method for producing polymer composites and used the PVA/h-BN additive. They compared the through-plane and in-plane thermal conductivities of the composites they made and reported that the in-plane thermal conductivity was higher than the through-plane [9]. Gou et al. produced 25% by volume randomly dispersed h-BN nanosheets/ Polyvinylidene fluoride-co-hexafluoropropylene (P(VDF-HFP)) nanocomposites and compared them with P(VDF-HFP) and the in-plane thermal conductivity of h-BN nanosheets/P(VDF-HFP) at 25% by volume-oriented increased by 249% and 3057%, respectively [10]. Sun et al. produced h-BN nanolayer-based epoxy nanocomposites. They emphasized that the thermal interface resistance is an essential factor preventing thermal conductivity along the plane and that the composites they produced have high xy/in-plane thermal conductivity and low thermal conductivity in z/plane [11]. Hu et al. reported that they obtained the highest through-plane thermal conductivity in the composite with 9.5% filler loading in the fluorinated h-BN nanolayers/graphene oxide elastomer composites they produced. Liu et al. simultaneously improved both in-plane and out-of-plane thermal conductivity in h-BN/polyimide composite films. They reported that the in-plane and out-of-plane thermal conductivity of the composite film with a filler content of 30% increased by 1233% and 150% compared to pure polyimide [12]. Zhang et al. achieved flexibility and high thermal conductivity in the through-plane direction in producing h-BN/polyethylene composites. They emphasized that they obtained mechanical properties and high thermal conductivity [13]. Hu et al. characterized oriented h-BN/Silicone rubber composites as the ideal thematic interface material. They stated that they managed to increase the thermal conductivity value of 7.62 W/mK while maintaining the flexibility of the composites they produced [14]. Su et al. produced composites with high thermal conductivity and good electrical insulation using multi-layer graphene and h-BN fillers with cycloaliphatic epoxy resin. Adding hybrid filler material to composite production has achieved high through-plane thermal conductivity [15]. Sun et al. calculate the effective thermal conductivity for in-plane and through-plane thermal conductivity for h-BN polymer composites modeled with the new anisotropic equation. The heat transfer is demonstrated by simulating the finite element method [16].

The process of gaining thermal conductivity characteristics and experimentally designing the desired high thermal conductivity composites, and researching the results is time-consuming and costly. However, since the phenomena that will occur at polymer composites'

interfaces and/or interphases cannot be fully demonstrated, the existing mechanism is investigated with theoretical and empirical models, numerical analyses, and simulations in the experimental study process [17]. Among the frequently preferred favorite models, the Russell model estimates the thermal conductivity of the composite structure by building a model on which the filling material is distributed in the matrix in the form of uniform cubes and in a regular manner. However, the Maxwell model [18] is particularly successful in predicting the thermal conductivity of composites with low-volume fractions. This model is because the model defined the filling material as spherical particles. Although the filling material could be in different geometries (shape factor n), it was the Hamilton-Crosser [19] who made improvements to the model. On the other hand, Nielsen's model [20] included more complex factors while creating the model structure with factors related to particle size and shape. For example, using the Einstein coefficient, he also included the factor related to the shape and orientation of the particles in the model structure. Agari [21], on the other hand, introduced two basic models, parallel and serial, in 1987 and predicted that existing models would be between these two basic models. While the parallel model determines the upper limit, the serial model determines the lower limit. Then, based on the hypothesis that the particles have a homogeneous distribution in the polymer, Agari added the C_1 constant, which is related to the crystallinity and crystalline size of the polymer, and the C_2 factor, in which the thermal conduction for the additive material is transmitted in the form of a network chain to the model. Among these models, Bruggeman's theoretical model [22] built a robust theoretical model based on the hypothesis that there is a mutual interaction between particles thanks to infinitesimal changes. Although it has a more complex structure than other models, unlike most theoretical models, it has high predictive power without including any factor or parameter in the model.

This study includes a mathematical prediction of thermal conductivity behavior of filled polymer composites. In this context, thermal conductivity behaviors of composites containing h-BN and MW-CNT fillers were investigated based on theoretical models. As a result, the Bruggeman model successfully predicted the thermal conductivity behavior of thermoplastic composites produced by selecting an interface compatibilizing agent between high-density polyethylene and filler materials in composite production.

2. Materials and Methods

2.1 Materials and Methods

For the current study, the thermal conductivity data of polymer composites were obtained from the reference paper

[23]. The volume fraction and thermal conductivity of the composites are given in Table 1. In experimental studies, 10-30% filling material by volume was added to high-density polyethylene composites. While h-BN is chosen as the primary filling material, it is seen that the synergy between h-BN and MW-CNT increases thermal conductivity by adding 3% MW-CNT for another group of composites.

2.2. Methods

2.2.1 Classical Theoretical Models

Many models based on macroscopic properties have been presented to predict the thermal behavior of materials with heterogeneous structures, such as filled polymer composites. Existing models are divided into theoretical and empirical models. Some famous theoretical models are given in Table 2 [24].

In the model equations in Table 2, the thermal conductivity of λ , λ_1 , and λ_2 composites are the thermal conductivity of a matrix (continuous phase) and filler (dispersive phase), respectively. v (%) is the volume fraction of particles. The Russell and Maxwell-Eucken models designed for low volume ratios are given in Equation 1 and 2, respectively. In addition, the Hamilton Crosser model (Eq.3) is represented by the shape factor n . All the theoretical models in Table 2 except the Bruggeman model (see Eq. 4) satisfy the λ equation. In the simplified version of the Bruggeman model, $(1-v)$ is located to the equation's left. Here, a simplified version of the current model has been made and reduced to its current form.

Table 1. Experimental data [23]

		Volume fractions (%)						
Fillers	CNT	-	-	-	3	3	3	-
	h-BN	10	20	30	7	17	27	-
Matrix	HDPE	90	80	70	90	80	70	100
Thermal conductivity (W/mK)		0.61	0.881	1.199	0.711	1.088	1.54	0.415

Table 2. Some theoretical models

Models	Equations	
Russell	$\lambda = \lambda_1 \frac{v^{\frac{2}{3}} + \frac{\lambda_1}{\lambda_2} (1 - v^{\frac{2}{3}})}{v^{\frac{2}{3}} - v + \frac{\lambda_1}{\lambda_2} (1 - v^{\frac{2}{3}})}$	(1)
Maxwell-Eucken	$\lambda = \lambda_1 \frac{2\lambda_1 + \lambda_2 + 2v(\lambda_2 - \lambda_1)}{2\lambda_1 + \lambda_2 - v(\lambda_2 - \lambda_1)}$	(2)
Hamilton-Crosser	$\lambda = \lambda_1 \left[\frac{\lambda_2 + (n-1)\lambda_1 + (n-1)v(\lambda_2 - \lambda_1)}{\lambda_2 + (n-1)\lambda_1 - v(\lambda_2 - \lambda_1)} \right]^n$	(3)
Bruggeman	$1 - v = \frac{\lambda_2 - \lambda}{\lambda_2 - \lambda_1} \left(\frac{\lambda_1}{\lambda} \right)^{1/3}$	(4)

However, the equation of the current model is in a rather lengthy form (in Appendix). When Appendix is examined, it is seen that there are 3 different solutions belonging to the Bruggeman model.

The first solution includes λ , λ_1 , λ_2 , and v in the Bruggeman model structure. At the same time, the imaginary number represented by i is also included in the other solutions. The current model has a very complex structure, which shows that it offers a strong structure among theoretical models. In addition, unlike models such as Hamilton-Crosser, Nielsen, and Agari, it is a model created in basic form without including various factors and parameters in its structure.

3. Results and Discussion

The thermal conductivity behaviors of H-BN/high-density polyethylene and h-BN/MW-CNT/high-density polyethylene composites were modeled with the theoretical Bruggeman model. It is essential to reduce agglomeration and provide the desired formation of the network structure in the production of composites in high-density polyethylene thermoplastic matrix with fillers such as BN and MW-CNT. For this, it is advantageous to add modifying maleic anhydride grafted high-density polyethylene, which is a famous compatibilizer agent in composite production [23]. In addition, the results of the measurements in the in-plane direction of the thermal conductivity of the composites are included in the study.

Figure 1 shows the model estimates of the thermal conductivity coefficient of the theoretical Bruggeman model for h-BN/high-density polyethylene composites. In addition, the average deviation values of the model are shown for each volume fraction in Table 3.

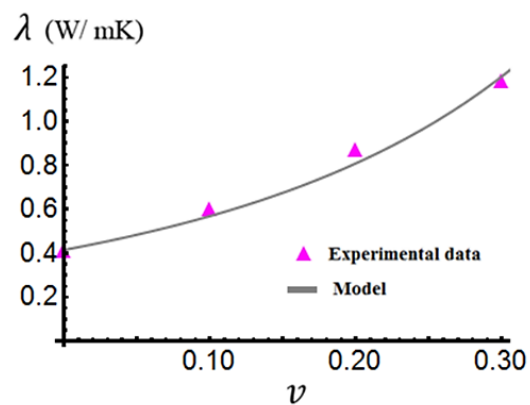


Figure 1. Bruggeman theoretical model prediction for h-BN/ high-density polyethylene composites

Table 3 The average deviation of the model estimate for h-BN/ high-density polyethylene composites

Volume fraction	Model
0.0	0.134
0.1	0.236
0.2	5.082
0.3	2.229

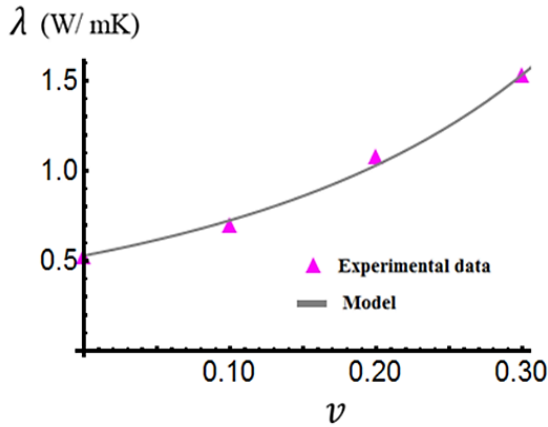


Figure 2. Bruggeman theoretical model prediction for h-BN/ MW-CNT/high-density polyethylene composites

Table 4 Average deviation of the model estimate for h-BN/MW-CNT/high-density polyethylene composites

Volume fraction	Model
0.0	0.134
0.1	2.136
0.2	3.082
0.3	0.229

The thermal conductivity of polyethylene composites increased together with the use of h-BN and MW-CNT fillers, which is attributed to the synergetic effect between the additives. The model estimates of the thermal conductivity coefficient of the theoretical Bruggeman model for h-BN/ MW-CNT/high-density polyethylene composites are shown in Figure 2. In addition, the mean deviation value of the model is presented in Table 4, including the data for all composites.

The Bruggeman model predicted the thermal conductivity behavior of h-BN/polyethylene and h-BN/MW-CNT/polyethylene composites with an accuracy of 97.8% and 99.4%, respectively. The average deviation values between the experimental data and the model predictions were calculated according to the volume fraction of each composite. The average deviation in filler ratios with 0, 10, 20, and 30 volume fractions are calculated as 0.134, 0.236, 5.082, and 2.229 for h-BN/polyethylene composites, and 0.134, 2.136, 3.082 for h-BN/MW-CNT/polyethylene composites. Model estimates gave better results for h-BN and h-BN/MW-CNT/polyethylene composites, especially at 0% and 30 volume fractions.

Figures 1 and 2 show a significant increase in thermal conductivity coefficient with additional MW-CNT in 20% and 30% by volume h-BN filled composites. This situation was interpreted as the synergistic effect between h-BN and MW-CNT. According to the experimental data, the thermal conductivity coefficients of the composites have a positive correlation. Additionally, the estimates of existing theoretical and empirical models have slopes that increase with increasing additive ratios.

3. Conclusion

In this study, the thermal conductivity of both h-BN and h-BN/MW-CNT filled composites was estimated using the Bruggeman theoretical model, and the strong prediction capability of the model was demonstrated. The Bruggeman theoretical model predicts the thermal conductivity of high-density polyethylene composites over $R^2 > 0.97$. The current model, which very well predicts the thermal conductivity of h-BN filled composites, perfectly predicts the thermal conductivity coefficients of h-BN/MW-CNT filled composites. However, since the phenomena that will occur at the interfaces and/or interphases of polymer composites cannot be fully revealed, it becomes essential to investigate the existing mechanism with theoretical and empirical models, numerical analyzes, and simulations in the experimental study process. Considering the long duration of the experimental process and the costs in the investigation of the thermal conductivity of composites, a numerical investigation utilizing theoretical models can give an idea about the existing mechanism.

Declaration

The author declared no potential conflicts of interest with respect to the research, authorship, and/or publication of this article. The author also declared that this article is original, was prepared in accordance with international publication and research ethics, and ethical committee permission or any special permission is not required.

Author Contributions

N. Kucukdogan developed the methodology, performed the analysis and wrote the whole article.

References

- Ruan, K., et al., *Interfacial thermal resistance in thermally conductive polymer composites: a review*. Composites Communications, 2020. **22**: p. 100518.
- Yang, X., et al., *A review on thermally conductive polymeric composites: classification, measurement, model and equations, mechanism and fabrication methods*. Advanced composites and hybrid materials, 2018. **1**(2): p. 207-230.
- Guo, Y., et al., *Factors affecting thermal conductivities of the polymers and polymer composites: A review*. Composites Science and Technology, 2020. **193**: p. 108134.
- Leung, S.N., *Thermally conductive polymer composites and nanocomposites: Processing-structure-property relationships*. Composites Part B: Engineering, 2018. **150**: p. 78-92.
- Liu, C., et al., *ZnO nanowire-decorated Al₂O₃ hybrids for improving the thermal conductivity of polymer composites*. Journal of Materials Chemistry C, 2020. **8**(16): p. 5380-5388.
- Cakmak, N.K., H.H. Durmazucar, and K. Yapici, *A numerical study of the natural convection of Al₂O₃-EG nanofluid in a square enclosure and impacts and a comparison of various viscosity and thermal conductivity*

models. International Advanced Researches and Engineering Journal, 2021. 5(2): p. 218-230.

7. Sanker, S.B. and R. Baby, *Phase change material based thermal management of lithium ion batteries: A review on thermal performance of various thermal conductivity enhancers*. Journal of Energy Storage, 2022. 50: p. 104606.
8. Jouni, M., et al., *A representative and comprehensive review of the electrical and thermal properties of polymer composites with carbon nanotube and other nanoparticle fillers*. Polymer International, 2017. 66(9): p. 1237-1251.
9. Zhang, J., et al., *A facile method to prepare flexible boron nitride/poly (vinyl alcohol) composites with enhanced thermal conductivity*. Composites Science and Technology, 2017. 149: p. 41-47.
10. Gou, B., et al., *Polymer-based nanocomposites with ultra-high in-plane thermal conductivity via highly oriented boron nitride nanosheets*. Polymer Composites, 2022. 43(4): p. 2341-2349.
11. Sun, Z., et al. *Large-scale production of boron nitride nanosheets-based epoxy nanocomposites with ultrahigh through-plane thermal conductivity for electronic encapsulation*. in 2022 IEEE 72nd Electronic Components and Technology Conference (ECTC). 2022. IEEE.
12. Liu, D., et al., *Improving in-plane and out-of-plane thermal conductivity of polyimide/boron nitride film with reduced graphene oxide by a moving magnetic field induction*. Composites Science and Technology, 2022. 220: p. 109292.
13. Zhang, R.C., et al., *Flexible and Ultrahigh Through-Plane Thermally-Conductive Polyethylene/Boron Nitride Nanocomposite Films*. Macromolecular Materials and Engineering, 2022. 307(1): p. 2100695.
14. Hu, Q., et al., *Oriented BN/Silicone rubber composite thermal interface materials with high out-of-plane thermal conductivity and flexibility*. Composites Part A: Applied Science and Manufacturing, 2022. 152: p. 106681.
15. Su, Z., et al., *Synergistic enhancement of anisotropic thermal transport flexible polymer composites filled with multi-layer graphene (mG) and mussel-inspired modified hexagonal boron nitride (h-BN)*. Composites Part A: Applied Science and Manufacturing, 2018. 111: p. 12-22.
16. Sun, Y., et al., *A new anisotropic thermal conductivity equation for h-BN/polymer composites using finite element analysis*. International Journal of Heat and Mass Transfer, 2020. 160: p. 120157.
17. Liu, B., et al., *Stochastic integrated machine learning based multiscale approach for the prediction of the thermal conductivity in carbon nanotube reinforced polymeric composites*. Composites Science and Technology, 2022. 224: p. 109425.
18. Maxwell, J.C., *A treatise on electricity and magnetism*. Vol. 1. 1881: Clarendon press.
19. Hamilton, R. and O. Crosser, *Thermal conductivity of heterogeneous two-component systems*. Industrial & Engineering chemistry fundamentals, 1962. 1(3): p. 187-191.
20. Nielsen, L.E., *Thermal conductivity of particulate-filled polymers*. Journal of applied polymer science, 1973. 17(12): p. 3819-3820.
21. Agari, Y., et al., *Thermal conductivity of a polymer composite filled with mixtures of particles*. Journal of Applied Polymer Science, 1987. 34(4): p. 1429-1437.
22. Bruggeman, V.D., *Berechnung verschiedener physikalischer Konstanten von heterogenen Substanzen. I. Dielektrizitätskonstanten und Leitfähigkeiten der*

Mischkörper aus isotropen Substanzen. Annalen der physik, 1935. 416(7): p. 636-664.

23. Feng, M., et al., *Largely improved thermal conductivity of HDPE composites by building a 3D hybrid fillers network*. Composites Science and Technology, 2021. 206: p. 108666.
24. Kucukdogan, N., L. Aydin, and M. Sutcu, *Theoretical and empirical thermal conductivity models of red mud filled polymer composites*. Thermochimica Acta, 2018. 665: p. 76-84.

Appendix

$$\{\lambda = \lambda_2 - (2^{1/3} (-9 \lambda_1^2 \lambda_2^2 + 3 \lambda_1 (\lambda_1^3 - 3 v \lambda_1^3 + 3 v^2 \lambda_1^3 - v^3 \lambda_1^3 - 3 \lambda_1^2 \lambda_2 + 9 v \lambda_1^2 \lambda_2 - 9 v^2 \lambda_1^2 \lambda_2 + 3 v^3 \lambda_1^2 \lambda_2 + 6 \lambda_1 \lambda_2^2 - 9 v \lambda_1 \lambda_2^2 + 9 v^2 \lambda_1 \lambda_2^2 - 3 v^3 \lambda_1 \lambda_2^2 - \lambda_2^3 + 3 v \lambda_2^3 - 3 v^2 \lambda_2^3 + v^3 \lambda_2^3)))/(3 \lambda_1 (-27 \lambda_1^5 \lambda_2 + 81 v \lambda_1^5 \lambda_2 - 81 v^2 \lambda_1^5 \lambda_2 + 27 v^3 \lambda_1^5 \lambda_2 + 81 \lambda_1^4 \lambda_2^2 - 243 v \lambda_1^4 \lambda_2^2 + 243 v^2 \lambda_1^4 \lambda_2^2 - 81 v^3 \lambda_1^4 \lambda_2^2 - 81 \lambda_1^3 \lambda_2^3 + 243 v \lambda_1^3 \lambda_2^3 - 243 v^2 \lambda_1^3 \lambda_2^3 + 81 v^3 \lambda_1^3 \lambda_2^3 + 27 \lambda_1^2 \lambda_2^4 - 81 v \lambda_1^2 \lambda_2^4 + 81 v^2 \lambda_1^2 \lambda_2^4 - 27 v^3 \lambda_1^2 \lambda_2^4 + \sqrt{((-27 \lambda_1^5 \lambda_2 + 81 v \lambda_1^5 \lambda_2 - 81 v^2 \lambda_1^5 \lambda_2 + 27 v^3 \lambda_1^5 \lambda_2 + 81 \lambda_1^4 \lambda_2^2 - 243 v \lambda_1^4 \lambda_2^2 + 243 v^2 \lambda_1^4 \lambda_2^2 - 81 v^3 \lambda_1^4 \lambda_2^2 - 81 \lambda_1^3 \lambda_2^3 + 243 v \lambda_1^3 \lambda_2^3 - 243 v^2 \lambda_1^3 \lambda_2^3 + 81 v^3 \lambda_1^3 \lambda_2^3 + 27 \lambda_1^2 \lambda_2^4 - 81 v \lambda_1^2 \lambda_2^4 + 81 v^2 \lambda_1^2 \lambda_2^4 - 27 v^3 \lambda_1^2 \lambda_2^4)^2 + (-9 \lambda_1^2 \lambda_2^2 + 3 \lambda_1 (\lambda_1^3 - 3 v \lambda_1^3 + 3 v^2 \lambda_1^3 - v^3 \lambda_1^3 - 3 \lambda_1^2 \lambda_2 + 9 v \lambda_1^2 \lambda_2 - 9 v^2 \lambda_1^2 \lambda_2 + 3 v^3 \lambda_1^2 \lambda_2 + 6 \lambda_1 \lambda_2^2 - 9 v \lambda_1 \lambda_2^2 + 9 v^2 \lambda_1 \lambda_2^2 - 3 v^3 \lambda_1 \lambda_2^2 - \lambda_2^3 + 3 v \lambda_2^3 - 3 v^2 \lambda_2^3 + v^3 \lambda_2^3))^3)}^{1/3}) + 1/(3 \cdot 2^{1/3} \lambda_1) (-27 \lambda_1^5 \lambda_2 + 81 v \lambda_1^5 \lambda_2 - 81 v^2 \lambda_1^5 \lambda_2 + 27 v^3 \lambda_1^5 \lambda_2 + 81 \lambda_1^4 \lambda_2^2 - 243 v \lambda_1^4 \lambda_2^2 + 243 v^2 \lambda_1^4 \lambda_2^2 - 81 v^3 \lambda_1^4 \lambda_2^2 - 81 \lambda_1^3 \lambda_2^3 + 243 v \lambda_1^3 \lambda_2^3 - 243 v^2 \lambda_1^3 \lambda_2^3 + 81 v^3 \lambda_1^3 \lambda_2^3 + 27 \lambda_1^2 \lambda_2^4 - 81 v \lambda_1^2 \lambda_2^4 + 81 v^2 \lambda_1^2 \lambda_2^4 - 27 v^3 \lambda_1^2 \lambda_2^4 + 4 (-9 \lambda_1^2 \lambda_2^2 + 3 \lambda_1 (\lambda_1^3 - 3 v \lambda_1^3 + 3 v^2 \lambda_1^3 - v^3 \lambda_1^3 - 3 \lambda_1^2 \lambda_2 + 9 v \lambda_1^2 \lambda_2 - 9 v^2 \lambda_1^2 \lambda_2 + 3 v^3 \lambda_1^2 \lambda_2 + 6 \lambda_1 \lambda_2^2 - 9 v \lambda_1 \lambda_2^2 + 9 v^2 \lambda_1 \lambda_2^2 - 3 v^3 \lambda_1 \lambda_2^2 - \lambda_2^3 + 3 v \lambda_2^3 - 3 v^2 \lambda_2^3 + v^3 \lambda_2^3))^3)}^{1/3}\}$$

$$\{\lambda = \lambda_2 + ((1 + i \sqrt{3}) (-9 \lambda_1^2 \lambda_2^2 + 3 \lambda_1 (\lambda_1^3 - 3 v \lambda_1^3 + 3 v^2 \lambda_1^3 - v^3 \lambda_1^3 - 3 \lambda_1^2 \lambda_2 + 9 v \lambda_1^2 \lambda_2 - 9 v^2 \lambda_1^2 \lambda_2 + 3 v^3 \lambda_1^2 \lambda_2 + 6 \lambda_1 \lambda_2^2 - 9 v \lambda_1 \lambda_2^2 + 9 v^2 \lambda_1 \lambda_2^2 - 3 v^3 \lambda_1 \lambda_2^2 - \lambda_2^3 + 3 v \lambda_2^3 - 3 v^2 \lambda_2^3 + v^3 \lambda_2^3)))/(3 \cdot 2^{2/3} \lambda_1 (-27 \lambda_1^5 \lambda_2 + 81 v \lambda_1^5 \lambda_2 - 81 v^2 \lambda_1^5 \lambda_2 + 27 v^3 \lambda_1^5 \lambda_2 + 81 \lambda_1^4 \lambda_2^2 - 243 v \lambda_1^4 \lambda_2^2 + 243 v^2 \lambda_1^4 \lambda_2^2 - 81 v^3 \lambda_1^4 \lambda_2^2 - 81 \lambda_1^3 \lambda_2^3 + 243 v \lambda_1^3 \lambda_2^3 - 243 v^2 \lambda_1^3 \lambda_2^3 + 81 v^3 \lambda_1^3 \lambda_2^3 + 27 \lambda_1^2 \lambda_2^4 - 81 v \lambda_1^2 \lambda_2^4 + 81 v^2 \lambda_1^2 \lambda_2^4 - 27 v^3 \lambda_1^2 \lambda_2^4 + \sqrt{((-27 \lambda_1^5 \lambda_2 + 81 v \lambda_1^5 \lambda_2 - 81 v^2 \lambda_1^5 \lambda_2 + 27 v^3 \lambda_1^5 \lambda_2 + 81 \lambda_1^4 \lambda_2^2 - 243 v \lambda_1^4 \lambda_2^2 + 243 v^2 \lambda_1^4 \lambda_2^2 - 81 v^3 \lambda_1^4 \lambda_2^2 - 81 \lambda_1^3 \lambda_2^3 + 243 v \lambda_1^3 \lambda_2^3 - 243 v^2 \lambda_1^3 \lambda_2^3 + 81 v^3 \lambda_1^3 \lambda_2^3 + 27 \lambda_1^2 \lambda_2^4 - 81 v \lambda_1^2 \lambda_2^4 + 81 v^2 \lambda_1^2 \lambda_2^4 - 27 v^3 \lambda_1^2 \lambda_2^4)^2 + 4 (-9 \lambda_1^2 \lambda_2^2 + 3 \lambda_1 (\lambda_1^3 - 3 v \lambda_1^3 + 3 v^2 \lambda_1^3 - v^3 \lambda_1^3 - 3 \lambda_1^2 \lambda_2 + 9 v \lambda_1^2 \lambda_2 - 9 v^2 \lambda_1^2 \lambda_2 + 3 v^3 \lambda_1^2 \lambda_2 + 6 \lambda_1 \lambda_2^2 - 9 v \lambda_1 \lambda_2^2 + 9 v^2 \lambda_1 \lambda_2^2 - 3 v^3 \lambda_1 \lambda_2^2 - \lambda_2^3 + 3 v \lambda_2^3 - 3 v^2 \lambda_2^3 + v^3 \lambda_2^3))^3)}^{1/3}) - 1/(6 \cdot 2^{1/3} \lambda_1) (1 - i \sqrt{3}) (-27 \lambda_1^5 \lambda_2 + 81 v \lambda_1^5 \lambda_2 - 81 v^2 \lambda_1^5 \lambda_2 + 27 v^3 \lambda_1^5 \lambda_2 + 81 \lambda_1^4 \lambda_2^2 - 243 v \lambda_1^4 \lambda_2^2 + 243 v^2 \lambda_1^4 \lambda_2^2 - 81 v^3 \lambda_1^4 \lambda_2^2 - 81 \lambda_1^3 \lambda_2^3 + 243 v \lambda_1^3 \lambda_2^3 - 243 v^2 \lambda_1^3 \lambda_2^3 + 81 v^3 \lambda_1^3 \lambda_2^3 + 27 \lambda_1^2 \lambda_2^4 - 81 v \lambda_1^2 \lambda_2^4 + 81 v^2 \lambda_1^2 \lambda_2^4 - 27 v^3 \lambda_1^2 \lambda_2^4 + \sqrt{((-27 \lambda_1^5 \lambda_2 + 81 v \lambda_1^5 \lambda_2 - 81 v^2 \lambda_1^5 \lambda_2 + 27 v^3 \lambda_1^5 \lambda_2 + 81 \lambda_1^4 \lambda_2^2 - 243 v \lambda_1^4 \lambda_2^2 + 243 v^2 \lambda_1^4 \lambda_2^2 - 81 v^3 \lambda_1^4 \lambda_2^2 - 81 \lambda_1^3 \lambda_2^3 + 243 v \lambda_1^3 \lambda_2^3 - 243 v^2 \lambda_1^3 \lambda_2^3 + 81 v^3 \lambda_1^3 \lambda_2^3 + 27 \lambda_1^2 \lambda_2^4 - 81 v \lambda_1^2 \lambda_2^4 + 81 v^2 \lambda_1^2 \lambda_2^4 - 27 v^3 \lambda_1^2 \lambda_2^4)^2 + 4 (-9 \lambda_1^2 \lambda_2^2 + 3 \lambda_1 (\lambda_1^3 - 3 v \lambda_1^3 + 3 v^2 \lambda_1^3 - v^3 \lambda_1^3 - 3 \lambda_1^2 \lambda_2 + 9 v \lambda_1^2 \lambda_2 - 9 v^2 \lambda_1^2 \lambda_2 + 3 v^3 \lambda_1^2 \lambda_2 + 6 \lambda_1 \lambda_2^2 - 9 v \lambda_1 \lambda_2^2 + 9 v^2 \lambda_1 \lambda_2^2 - 3 v^3 \lambda_1 \lambda_2^2 - \lambda_2^3 + 3 v \lambda_2^3 - 3 v^2 \lambda_2^3 + v^3 \lambda_2^3))^3)}^{1/3}\}$$

$$\{\lambda = \lambda_2 + ((1 - i \sqrt{3}) (-9 \lambda_1^2 \lambda_2^2 + 3 \lambda_1 (\lambda_1^3 - 3 v \lambda_1^3 + 3 v^2 \lambda_1^3 - v^3 \lambda_1^3 - 3 \lambda_1^2 \lambda_2 + 9 v \lambda_1^2 \lambda_2 - 9 v^2 \lambda_1^2 \lambda_2 + 3 v^3 \lambda_1^2 \lambda_2 + 6 \lambda_1 \lambda_2^2 - 9 v \lambda_1 \lambda_2^2 + 9 v^2 \lambda_1 \lambda_2^2 - 3 v^3 \lambda_1 \lambda_2^2 - \lambda_2^3 + 3 v \lambda_2^3 - 3 v^2 \lambda_2^3 + v^3 \lambda_2^3)))/(3 \cdot 2^{2/3} \lambda_1 (-27 \lambda_1^5 \lambda_2 + 81 v \lambda_1^5 \lambda_2 - 81 v^2 \lambda_1^5 \lambda_2 + 27 v^3 \lambda_1^5 \lambda_2 + 81 \lambda_1^4 \lambda_2^2 - 243 v \lambda_1^4 \lambda_2^2 + 243 v^2 \lambda_1^4 \lambda_2^2 - 81 v^3 \lambda_1^4 \lambda_2^2 - 81 \lambda_1^3 \lambda_2^3 + 243 v \lambda_1^3 \lambda_2^3 - 243 v^2 \lambda_1^3 \lambda_2^3 + 81 v^3 \lambda_1^3 \lambda_2^3 + 27 \lambda_1^2 \lambda_2^4 - 81 v \lambda_1^2 \lambda_2^4 + 81 v^2 \lambda_1^2 \lambda_2^4 - 27 v^3 \lambda_1^2 \lambda_2^4 + \sqrt{((-27 \lambda_1^5 \lambda_2 + 81 v \lambda_1^5 \lambda_2 - 81 v^2 \lambda_1^5 \lambda_2 + 27 v^3 \lambda_1^5 \lambda_2 + 81 \lambda_1^4 \lambda_2^2 - 243 v \lambda_1^4 \lambda_2^2 + 243 v^2 \lambda_1^4 \lambda_2^2 - 81 v^3 \lambda_1^4 \lambda_2^2 - 81 \lambda_1^3 \lambda_2^3 + 243 v \lambda_1^3 \lambda_2^3 - 243 v^2 \lambda_1^3 \lambda_2^3 + 81 v^3 \lambda_1^3 \lambda_2^3 + 27 \lambda_1^2 \lambda_2^4 - 81 v \lambda_1^2 \lambda_2^4 + 81 v^2 \lambda_1^2 \lambda_2^4 - 27 v^3 \lambda_1^2 \lambda_2^4)^2 + 4 (-9 \lambda_1^2 \lambda_2^2 + 3 \lambda_1 (\lambda_1^3 - 3 v \lambda_1^3 + 3 v^2 \lambda_1^3 - v^3 \lambda_1^3 - 3 \lambda_1^2 \lambda_2 + 9 v \lambda_1^2 \lambda_2 - 9 v^2 \lambda_1^2 \lambda_2 + 3 v^3 \lambda_1^2 \lambda_2 + 6 \lambda_1 \lambda_2^2 - 9 v \lambda_1 \lambda_2^2 + 9 v^2 \lambda_1 \lambda_2^2 - 3 v^3 \lambda_1 \lambda_2^2 - \lambda_2^3 + 3 v \lambda_2^3 - 3 v^2 \lambda_2^3 + v^3 \lambda_2^3))^3)}^{1/3}) - 1/(6 \cdot 2^{1/3} \lambda_1) (1 - i \sqrt{3}) (-27 \lambda_1^5 \lambda_2 + 81 v \lambda_1^5 \lambda_2 - 81 v^2 \lambda_1^5 \lambda_2 + 27 v^3 \lambda_1^5 \lambda_2 + 81 \lambda_1^4 \lambda_2^2 - 243 v \lambda_1^4 \lambda_2^2 + 243 v^2 \lambda_1^4 \lambda_2^2 - 81 v^3 \lambda_1^4 \lambda_2^2 - 81 \lambda_1^3 \lambda_2^3 + 243 v \lambda_1^3 \lambda_2^3 - 243 v^2 \lambda_1^3 \lambda_2^3 + 81 v^3 \lambda_1^3 \lambda_2^3 + 27 \lambda_1^2 \lambda_2^4 - 81 v \lambda_1^2 \lambda_2^4 + 81 v^2 \lambda_1^2 \lambda_2^4 - 27 v^3 \lambda_1^2 \lambda_2^4 + \sqrt{((-27 \lambda_1^5 \lambda_2 + 81 v \lambda_1^5 \lambda_2 - 81 v^2 \lambda_1^5 \lambda_2 + 27 v^3 \lambda_1^5 \lambda_2 + 81 \lambda_1^4 \lambda_2^2 - 243 v \lambda_1^4 \lambda_2^2 + 243 v^2 \lambda_1^4 \lambda_2^2 - 81 v^3 \lambda_1^4 \lambda_2^2 - 81 \lambda_1^3 \lambda_2^3 + 243 v \lambda_1^3 \lambda_2^3 - 243 v^2 \lambda_1^3 \lambda_2^3 + 81 v^3 \lambda_1^3 \lambda_2^3 + 27 \lambda_1^2 \lambda_2^4 - 81 v \lambda_1^2 \lambda_2^4 + 81 v^2 \lambda_1^2 \lambda_2^4 - 27 v^3 \lambda_1^2 \lambda_2^4)^2 + 4 (-9 \lambda_1^2 \lambda_2^2 + 3 \lambda_1 (\lambda_1^3 - 3 v \lambda_1^3 + 3 v^2 \lambda_1^3 - v^3 \lambda_1^3 - 3 \lambda_1^2 \lambda_2 + 9 v \lambda_1^2 \lambda_2 - 9 v^2 \lambda_1^2 \lambda_2 + 3 v^3 \lambda_1^2 \lambda_2 + 6 \lambda_1 \lambda_2^2 - 9 v \lambda_1 \lambda_2^2 + 9 v^2 \lambda_1 \lambda_2^2 - 3 v^3 \lambda_1 \lambda_2^2 - \lambda_2^3 + 3 v \lambda_2^3 - 3 v^2 \lambda_2^3 + v^3 \lambda_2^3))^3)}^{1/3}\}$$

$$\begin{aligned}
& \lambda_2^3)) / (3 \cdot 2^{2/3} \lambda_1 (-27 \lambda_1^5 \lambda_2 + 81 v \lambda_1^5 \lambda_2 - 81 v^2 \lambda_1^5 \lambda_2 + 27 v^3 \lambda_1^5 \\
& \lambda_2 + 81 \lambda_1^4 \lambda_2^2 - 243 v \lambda_1^4 \lambda_2^2 + 243 v^2 \lambda_1^4 \lambda_2^2 - 81 v^3 \lambda_1^4 \lambda_2^2 - 81 \\
& \lambda_1^3 \lambda_2^3 + 243 v \lambda_1^3 \lambda_2^3 - 243 v^2 \lambda_1^3 \lambda_2^3 + 81 v^3 \lambda_1^3 \lambda_2^3 + 27 \lambda_1^2 \lambda_2^4 \\
& - 81 v \lambda_1^2 \lambda_2^4 + 81 v^2 \lambda_1^2 \lambda_2^4 - 27 v^3 \lambda_1^2 \lambda_2^4 + \sqrt{((-27 \lambda_1^5 \lambda_2 + 81 v \\
& \lambda_1^5 \lambda_2 - 81 v^2 \lambda_1^5 \lambda_2 + 27 v^3 \lambda_1^5 \lambda_2 + 81 \lambda_1^4 \lambda_2^2 - 243 v \lambda_1^4 \lambda_2^2 + 243 \\
& v^2 \lambda_1^4 \lambda_2^2 - 81 v^3 \lambda_1^4 \lambda_2^2 - 81 \lambda_1^3 \lambda_2^3 + 243 v \lambda_1^3 \lambda_2^3 - 243 v^2 \lambda_1^3 \lambda_2^3 \\
& + 81 v^3 \lambda_1^3 \lambda_2^3 + 27 \lambda_1^2 \lambda_2^4 - 81 v \lambda_1^2 \lambda_2^4 + 81 v^2 \lambda_1^2 \lambda_2^4 - 27 v^3 \lambda_1^2 \\
& \lambda_2^4)^2 + 4 (-9 \lambda_1^2 \lambda_2^2 + 3 \lambda_1 (\lambda_1^3 - 3 v \lambda_1^3 + 3 v^2 \lambda_1^3 - v^3 \lambda_1^3 - 3 \lambda_1^2 \\
& \lambda_2 + 9 v \lambda_1^2 \lambda_2 - 9 v^2 \lambda_1^2 \lambda_2 + 3 v^3 \lambda_1^2 \lambda_2 + 6 \lambda_1 \lambda_2^2 - 9 v \lambda_1 \lambda_2^2 + 9 \\
& v^2 \lambda_1 \lambda_2^2 - 3 v^3 \lambda_1 \lambda_2^2 - \lambda_2^3 + 3 v \lambda_2^3 - 3 v^2 \lambda_2^3 + v^3 \lambda_2^3))^3})^{1/3} - \\
& 1 / (6 \cdot 2^{1/3} \lambda_1) (1 + i \sqrt{3}) (-27 \lambda_1^5 \lambda_2 + 81 v \lambda_1^5 \lambda_2 - 81 v^2 \lambda_1^5 \lambda_2 + 27 \\
& v^3 \lambda_1^5 \lambda_2 + 81 \lambda_1^4 \lambda_2^2 - 243 v \lambda_1^4 \lambda_2^2 + 243 v^2 \lambda_1^4 \lambda_2^2 - 81 v^3 \lambda_1^4 \lambda_2^2 \\
& - 81 \lambda_1^3 \lambda_2^3 + 243 v \lambda_1^3 \lambda_2^3 - 243 v^2 \lambda_1^3 \lambda_2^3 + 81 v^3 \lambda_1^3 \lambda_2^3 + 27 \lambda_1^2 \\
& \lambda_2^4 - 81 v \lambda_1^2 \lambda_2^4 + 81 v^2 \lambda_1^2 \lambda_2^4 - 27 v^3 \lambda_1^2 \lambda_2^4 + \sqrt{((-27 \lambda_1^5 \lambda_2 + \\
& 81 v \lambda_1^5 \lambda_2 - 81 v^2 \lambda_1^5 \lambda_2 + 27 v^3 \lambda_1^5 \lambda_2 + 81 \lambda_1^4 \lambda_2^2 - 243 v \lambda_1^4 \lambda_2^2 \\
& + 243 v^2 \lambda_1^4 \lambda_2^2 - 81 v^3 \lambda_1^4 \lambda_2^2 - 81 \lambda_1^3 \lambda_2^3 + 243 v \lambda_1^3 \lambda_2^3 - 243 v^2 \\
& \lambda_1^3 \lambda_2^3 + 81 v^3 \lambda_1^3 \lambda_2^3 + 27 \lambda_1^2 \lambda_2^4 - 81 v \lambda_1^2 \lambda_2^4 + 81 v^2 \lambda_1^2 \lambda_2^4 - 27 \\
& v^3 \lambda_1^2 \lambda_2^4)^2 + 4 (-9 \lambda_1^2 \lambda_2^2 + 3 \lambda_1 (\lambda_1^3 - 3 v \lambda_1^3 + 3 v^2 \lambda_1^3 - v^3 \lambda_1^3 - 3 \\
& \lambda_1^2 \lambda_2 + 9 v \lambda_1^2 \lambda_2 - 9 v^2 \lambda_1^2 \lambda_2 + 3 v^3 \lambda_1^2 \lambda_2 + 6 \lambda_1 \lambda_2^2 - 9 v \lambda_1 \lambda_2^2 + \\
& 9 v^2 \lambda_1 \lambda_2^2 - 3 v^3 \lambda_1 \lambda_2^2 - \lambda_2^3 + 3 v \lambda_2^3 - 3 v^2 \lambda_2^3 + v^3 \lambda_2^3))^3})^{1/3} \}
\end{aligned}$$